Reference: *Biol. Bull.* **209:** 21–30. (August 2005)

Polar Body Formation in *Spisula* Oocytes: Function of the Peripheral Aster

RAFAL M. PIELAK, CHRISTOPHER HAWKINS, AUNG PYIE, JENNIFER BAUTISTA, KYENG-GEA LEE, AND WILLIAM D. COHEN*

Department of Biological Sciences, Hunter College, New York, New York, and the Marine Biological Laboratory, Woods Hole, Massachusetts

Abstract. Activated *Spisula* oocytes proceed through meiotic stages rapidly and in near synchrony, providing an excellent system for analyzing polar body formation. Our previous studies suggested that cortical spreading of the metaphase peripheral aster determines spatial features of the cortical F-actin ring that is generated prior to extrusion of the polar body. We tested this hypothesis by experimentally altering the number and cortical contact patterns of peripheral asters. Such alteration was achieved by (a) lovastatin-induced arrest at metaphase I, with and without hexylene glycol modification, followed by washout; and (b) cytochalasin-D inhibition of extrusion of the first polar body, with washout before extrusion of the second polar body. Both methods induced simultaneous formation of two or more cortically spreading asters, correlated with subsequent formation of double, or even triple, overlapping F-actin rings during anaphase. Regardless of pattern, ring F-actin was deposited near regions of greatest astral microtubule density, indicating that microtubules provided a positive stimulus to which the cortex responded indiscriminately. These results strongly support the proposed causal relationship between peripheral aster spreading and biogenesis of the F-actin ring involved in polar body formation.

Introduction

Polar body (PB) formation is common to all sexually reproducing animals, but many details of this critical process and its products remain to be elucidated. We do not know the extent to which the mechanisms involved in generating such extreme asymmetry resemble those of normal somatic cell division, or whether these mechanisms are the same in all animals. Moreover, demonstrations of such fundamental features as PB division (Saiki and Hamaguchi, 1997), the PB F-actin ring pattern (Pielak *et al.,* 2003, 2004), Aurora kinase involvement in PB extrusion (Schumacher *et al.,* 1998; Castro *et al.,* 2003), and cytoskeletal differences between PB1 and PB2 (Alliegro and Alliegro, 2005) are relatively recent.

This paper addresses one major step in PB formation: deposition of the F-actin ring involved in PB extrusion. For this work we used *Spisula solidissima,* the large "surf clam" found in the eastern United States—an organism whose commercial importance (Weinberg and Helser, 1996) is more than matched by its value in biomedical research. *Spisula* is a prodigious gamete producer, and ripe animals retain viable eggs and sperm for several months if maintained at appropriate temperatures. Shed oocytes can be kept viable for at least 2 days (Hunt *et al.,* 1992), remaining at the germinal vesicle stage—prophase of meiosis I—until activated by sperm, KCl, or other agents (Allen, 1953; Longo *et al.,* 1991). Activated oocytes proceed through meiotic stages in near synchrony, including germinal vesicle breakdown (GVBD), formation of the metaphase I meiotic apparatus, translocation of the metaphase I spindle to the cortex, completion of meiosis I with extrusion of PB1, formation of the meiosis II spindle, and completion of meiosis II with PB2 extrusion. This entire sequence occurs in about 30 min under laboratory conditions (Allen, 1953) and is followed, in sperm-activated oocytes, by nuclear fusion and embryogenesis. Thus, *Spisula* gametes have served in studies of the meiotic cell cycle (Swenson *et al.,* 1987; Hunt *et al.,* 1992; Katsu *et al.,* 1999; Yi *et al.,* 2002; Dube and Eckberg, 1997) and in related work on the organization, function, molecular composition, and biogenesis

Received 18 March 2005; accepted 16 May 2005.

* To whom correspondence should be addressed. E-mail: cohen@genectr.hunter.cuny.edu or bcohen@mbl.edu

Abbreviations: CD, cytochalasin-D; GVBD, germinal vesicle breakdown; HG, hexylene glycol; LV, lovastatin; PB, polar body; PB1 and PB2, first and second polar bodies.

of centrosomes (Wu and Palazzo, 1999; Schnackenberg *et al.,* 2000), meiotic apparatus (Suprenant and Rebhun, 1984; Haimo, 1985; Kuriyama *et al.,* 1986; Suddith *et al.,* 2001), nuclear envelope (Maul *et al.,* 1987; Dessev and Goldman, 1988; Dessev et al., 1989), and PBs (Longo and Anderson, 1970; Pielak *et al.,* 2003, 2004; Alliegro and Alliegro, 2005). One deficiency recognized in recent years, a lack of genetic data for the species, is currently being addressed (Marine Biological Laboratory, 2003).

In previous work on cytoskeletal events during PB formation in *Spisula* (Pielak *et al.,* 2003, 2004), we found that the metaphase I peripheral aster spread onto the cortex in a circular pattern containing relatively few central microtubules. This aster disassembled during anaphase, and a ring of thickened F-actin appeared that had essentially the same cortical location, dimensions, and pattern as did microtubules in the earlier aster. The late anaphase spindle remained docked at the F-actin-poor center of the ring (the "ring opening"), where PB extrusion then occurred. The observed spatial correspondence immediately suggested that microtubules of the peripheral aster are a causal agent in generation of the PB F-actin ring.

The present studies were designed to test this hypothesis by altering the number of peripheral asters and their cortical contact patterns prior to PB formation. Two methods were employed. First, exposure to lovastatin (LV), followed by washout, induced both metaphase arrest (Turner *et al.,* 1995) and multiple asters under our conditions, an effect modified and enhanced by hexylene glycol (HG; Rebhun and Sawada, 1969; Saiki and Hamaguchi, 1997). Second, cytochalasin D (CD) was used to block PB1 extrusion, with extra asters being generated following washout prior to meiosis II (Longo, 1972; Hertzler, 2002). Both approaches gave strikingly consistent positive results, producing multiple peripheral asters associated with multiple, overlapping F-actin rings.

Materials and Methods

Ripe individuals of *Spisula solidissima* (Dillwyn, 1817), maintained at 11–13 °C to inhibit spawning, were obtained from the Aquatic Resources Division of the Marine Biological Laboratory (MBL) in Woods Hole, Massachusetts. Gonadal tissue was removed by dissection and suspended in about 150–300 ml of filtered (Whatman #2) natural seawater (F-NSW) depending on gonad size. After tissue removal by filtration through a double cheesecloth layer, the egg suspension passing through was allowed to settle (≈20–30 min), the supernate was removed, and the eggs were washed twice more by resuspension and settling. After determining approximate total egg volume by gentle hand-centrifugation, final resuspension was in F-NSW refiltered at 0.45-μm (= double-filtered, or DF-NSW) to a concentration of about 1% (v/v). Eggs were stored at this concentration in DF-NSW containing 50 μg/ml gentamycin (Hunt *et al.,* 1992), maintained in suspension at 16 °C in a rocking water bath. Such eggs retained the capacity for normal PB formation and (when sperm-activated) normal cleavage, but were used for 2 days only because, beyond that, increased time to PB formation suggested some deterioration.

Spisula oocytes were activated by using excess KCl, a standard method for this species (Allen, 1953; Costello and Henley, 1971). Eggs were gently hand-centrifuged and resuspended to 10% (v/v) in DF-NSW, and one volume of suspension was mixed with 7.6 vol. DF-NSW and 1.4 vol. 0.5 *M* KCl ($t = 0$). Eggs were monitored in phase contrast for GVBD, sedimented gently, resuspended in DF-NSW or experimental media to about 1% (v/v), and maintained in suspension by gentle rocking on a nutator at 22 °C. Samples were treated as described in particular experiments and then prepared for fluorescence labeling and microscopy (see below). The timing of stages became slightly extended with longer-term storage of ripe animals in cold seawater, and this was adjusted for by monitoring a range of time-point samples in each preparation.

Fluorescence labeling and microscopy

For rapid monitoring of chromosomal stage, oocytes were routinely fixed in seawater containing 2% or 4% formaldehyde (equally effective), stained with DAPI (3 or 6 μM), and examined and photographed using a standard Zeiss epifluorescence microscope. For cytoskeletal labeling, oocytes were simultaneously permeabilized and fixed for 15 min in PEM (100 m*M* PIPES, 5 m*M* EGTA, 1 m*M* $MgCl_2$, pH 6.8, using NaOH) containing 0.6% Brij-58 and 2% formaldehyde, then washed twice in phosphate-buffered saline (PBS). Labeling was performed in PBS using the following agents: for F-actin, Alexa Fluor 568-phalloidin (Molecular Probes); for microtubules, a mixture of mouse monoclonal anti-α and anti-β tubulins (Sigma T9026, T-4026) at their recommended working dilutions, pretagged with Alexa Fluor 488-labeled anti-mouse Fab fragments (Zenon; Molecular Probes); for DNA, DAPI. Labeling protocols were as described in prior work, without vitelline membrane removal (Lee *et al.,* 2002; Pielak *et al.,* 2003, 2004). Samples were viewed both in a standard Zeiss epifluorescence microscope and by confocal fluorescence microscopy using the Zeiss Laser Scanning System LSM 5 PASCAL, with image processing *via* Zeiss LSM Image Examiner (2004) and Adobe Photoshop (vers. 3.0) software. Aster or ring diameters were measured on images of optimum clarity, using Zeiss Image Examiner software. Relative pixel intensity was measured on the original 3-D reconstructed image in face view, using the Scion Image PC version of NIH-Image software (beta vers. 4.0.2).

Treatment with aster-perturbing agents

Following activation, *Spisula* oocytes proceed continuously from GVBD through meiosis and the extrusion of two

PBs. Therefore, we tested lovastatin (LV; Calbiochem) as a possible means to provide a time window for addition of aster-perturbing agents such as hexylene glycol (HG) that require oocyte penetration. LV, a 3-hydroxy-3-methylglutaryl coenzyme A reductase inhibitor, induces reversible metaphase I arrest of KCl-activated *Spisula* oocytes (Turner *et al.,* 1995). Using DF-NSW as the primary medium, as for other experimental agents and solvent controls described below, activated oocytes were incubated in LV at 3.5 μM, 35 μM, 52.5 μM, and 70 μM. Under our conditions, metaphase stability was most repeatable at 52.5 μM (1.5 $\times$ conc. used by Turner *et al.,* 1995), and this concentration was used routinely at about 12 min post-activation, when metaphase spindles were still centrally located and en route to the cortex. Solvent-only controls were exposed to 0.15% DMSO in DF-NSW. Oocyte samples were processed for fluorescence microscopy after various LV incubation periods before washout and during meiotic resumption after two washes in DF-NSW.

Hexylene glycol (HG, = 2-methyl-2,4-pentanediol; Sigma) reversibly increases aster size and stability (*Spisula:* Rebhun and Sawada, 1969; starfish: Saiki and Hamaguchi, 1997). During LV-induced metaphase time windows, HG (1% v/v) was added either "early" at $t = 20$ min post-activation, with $t = 25$ min washout (5 min HG incubation), or "late" at $t = 25$ or 30 min, with washout at 35 or 42 min, respectively (10 or 12 min HG incubation). Both late addition times gave the same results, so that HG use is described below as either early or late. For all experiments with LV plus HG, maximum oocyte exposure to LV was thus 30 min.

As in previous work (Pielak *et al.,* 2004), cytochalasin D (CD; Calbiochem) was used to inhibit F-actin ring assembly prior to PB1 formation. Eggs were sedimented gently and resuspended in 1.0 μg/ml CD or 0.1% DMSO (solvent control) at about 15 min post-activation, when metaphase spindles were still in transit to the cortex. Various times for initiating CD washout were then tested to determine which would block extrusion of PB1 while permitting that of PB2. Washout when solvent-only controls were still in metaphase ($\approx$20 min) was too early, allowing sequential formation of both PBs. Washout when controls were at late anaphase ($\approx$27–30 min) was too late; no PBs formed, and oocytes contained four pronuclei. However, washout with controls at anaphase onset ($\approx$25 min post-activation) permitted subsequent PB2 formation and was used in the experiments.

Results

F-actin ring formation in untreated oocytes

In the normal cytoskeletal sequence that precedes PB formation, the metaphase meiotic spindle moved toward the egg surface, the peripheral aster spread fountain-like onto the oocyte cortex, and subsequently in anaphase, most astral microtubules disassembled (Fig. 1A–C). The F-actin ring appeared in the cortical location of the previously spread aster, with similar outer diameter ($\approx$20–22 μm), and with the spindle docked at the center of the F-actin-deficient ring opening (Fig. 1C, D). Rotated 3-D reconstructions of cortical F-actin from optical section stacks revealed the circular pattern of the ring, with chromosomes positioned in the ring opening (Fig. 1E).

The normal pattern of F-actin deposition was also observed in solvent-only controls (Fig. 1F, G), again with an outer ring diameter of about 21–22 μm, as measured in optical sections of three rings. Thus, for comparison with the normal pattern, altered cortical F-actin deposition is described throughout this paper in terms of the "ring" and "ring opening." As examined in scans of pixel intensity across the ring, cortical F-actin was most dense within the ring, and the level in the ring opening resembled that of surrounding cortex (Fig. 1H).

Lovastatin-induced metaphase arrest, followed by washout

Lovastatin (LV) was initially tested to determine its utility in providing a time window for administration of hexylene glycol (HG) by means of metaphase arrest. First, we confirmed LV-induced metaphase arrest (Fig. 2A, B), as well as PB production in about 90% of oocytes after 30 min arrest and washout (Fig. 2C, D). However, we were surprised to discover that, under our conditions, LV-induced metaphase arrest lasted only about 30 min, after which anaphase began even without washout. More importantly for our objectives, most of the LV-treated oocytes displayed multiple asters with interconnected spindles (Fig. 2E). In a majority of oocytes, only one of these asters was in contact with the cortex; but in about 15%–20%, the meiotic apparatus was oriented such that two or three asters touched the cortex. In anaphase, such oocytes contained adjacent docked spindles (Fig. 2F) that were associated either with a single enlarged, circular or avoid F-actin ring ($>$30 μm; Fig. 2G) or with double F-actin rings (Fig. 2H–J). Each ring opening was occupied by a spindle centrosomal region (*e.g.,* Fig. 2H, J), and dual ring openings shared a strip of thickened F-actin between them that varied in width in different oocytes (*e.g.,* Fig. 2H–J).

Hexylene glycol addition during lovastatin metaphase arrest

Given the LV results, we tested HG addition during LV-induced time windows to determine whether it would increase astral cortical contact, enhancing or modifying the formation of multiple rings (Fig. 3). Astral spreading occurred during metaphase, as previously (Fig. 3A), and multiple spreading asters were observed (Fig. 3B). Two centrosomes were clearly present at the docking pole of some metaphase or early anaphase spindles (Fig. 3C). Single enlarged rings were most evident when HG was added

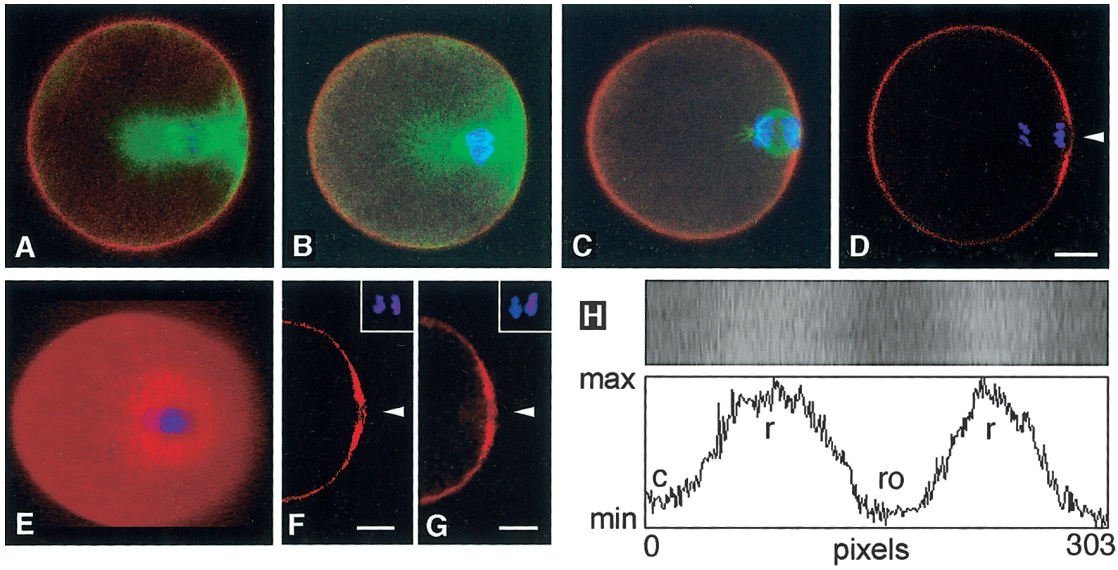

Figure 1. Cytoskeletal features preceding polar body formation in normal oocytes and in DMSO solvent controls (optical sections unless otherwise noted; microtubules, green; F-actin, red; chromosomes, blue-violet). (A) Docked metaphase spindle, with spreading peripheral aster. (B) Early anaphase spindle with spread aster. (C) Anaphase spindle abutting cortex at the ring center after most peripheral aster microtubules have disassembled. (D) Another anaphase oocyte, microtubules omitted. One chromosome set is centered at the ring opening (arrowhead). (E) Rotated 3-D view of the F-actin ring in the oocyte shown in (D), constructed from an image stack, illustrating the ≈22-μm-diameter ring pattern and chromosome location in the ring opening. (F, G) Optical sections of solvent-only control oocytes (0.15% DMSO), with same ≈20-μm-diameter ring pattern as in oocytes without solvent (arrowheads at ring opening). (H) Upper: face-view grayscale image of F-actin only, in rectangular area across the ring in (E); Lower: scan of pixel intensity in upper image; level in the ring opening (ro) is similar to that in the cortex (c) surrounding the ring (r). (A, B, D) From Pielak *et al.* (2003). Scale bars: 10 μm (bars for A–C and E, as in D).

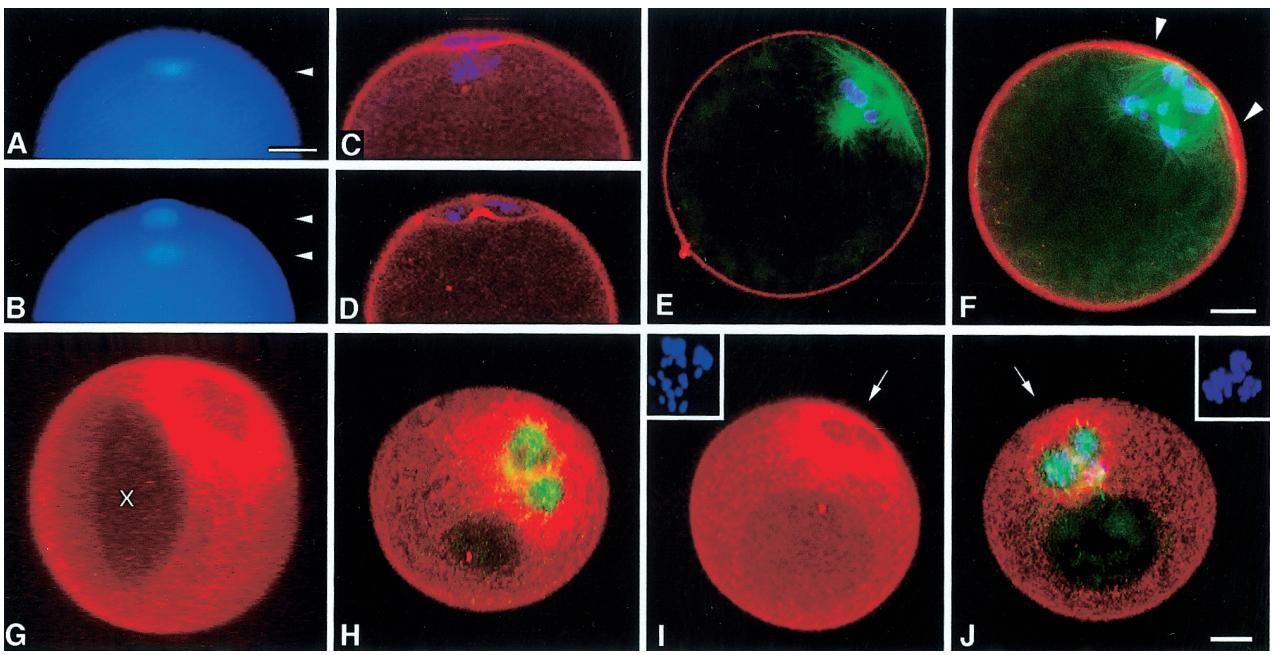

Figure 2. Lovastatin LV-induced formation of enlarged and multiple spreading asters, with subsequent cortical induction of enlarged F-actin rings. (A, B) Rapid DAPI labeling of chromosome sets (arrowheads) in metaphase and anaphase, respectively. (C, D) Optical sections showing polar body formation following lovastatin washout. (E) Docked duplex metaphase spindle, with very large spreading aster region, prior to F-actin deposition and polar body formation. (F) Peripheral centrosomes of two late anaphase spindles docked close together at the cortex. Note adjacent regions of thickened cortical F-actin (arrowheads). (G) Same oocyte, rotated 3-D view showing a single enlarged, ovoid F-actin ring and ring center (long axis of ≈35 μm). (H) Oocyte with large region of thickened cortical F-actin, centrosomes occupying the two ring openings, and a shared F-actin segment between them. (I) Another pattern, similar to (H), but with a much thinner inter-ring segment (arrow). Inset: chromosomes of same egg; the two upper chromosome groups were adjacent to the two ring openings. (J) Another oocyte with a dual ring pattern; inter-ring segment is intermediate in thickness between that of (H) and (I). Inset: chromosomes of same egg; the two upper left chromosome groups were adjacent to the two ring openings. NOTE: optical sectioning was restricted to the most relevant regions to limit photobleaching; unsectioned areas appear in some 3-D reconstructions (*e.g.,* area "x" in G). Scale bars: 10 μm (bar for B–D as in A; E and G as in F; H and I as in J).

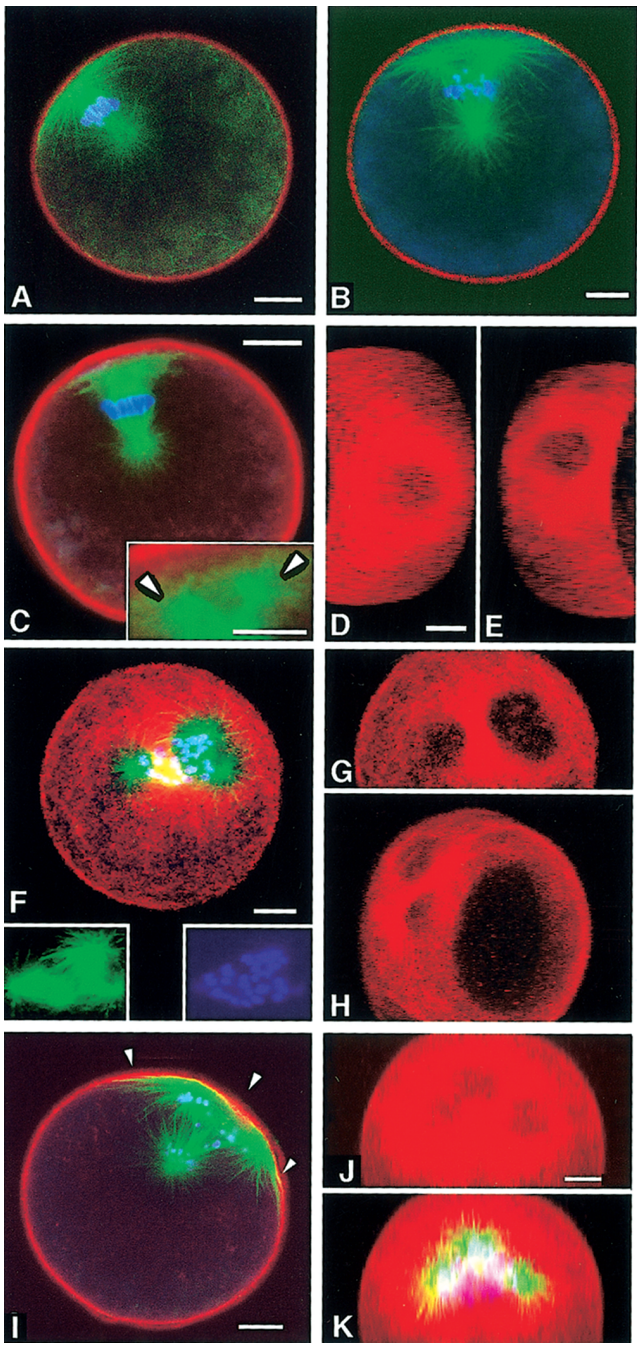

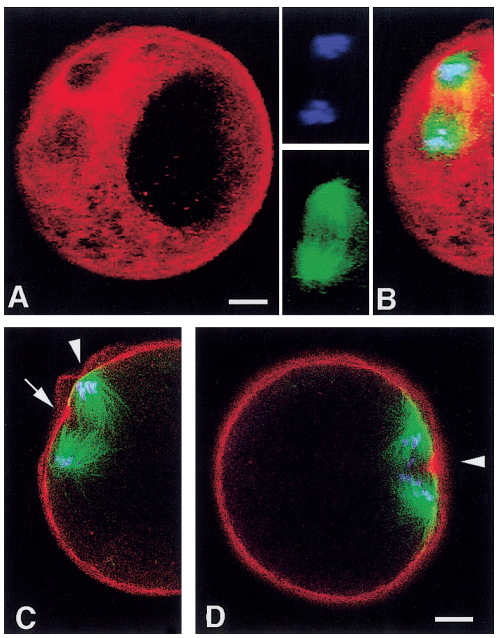

Figure 4. Spindle malorientation induced by lovastatin plus hexylene glycol: the spindle, normally perpendicular to the cortical surface, as in Fig. 1C, here is parallel. (A) Rotated 3-D view of anaphase cortical F-actin pattern. Upper inset: anaphase chromosome sets; lower inset: centrosomes of the two asters. (B) Composite of A + A insets. (C) Optical section of same cell, showing increased F-actin deposition between the ring openings (arrow), and edge view of one of the cortically docked spindle poles (arrowhead). (D) Optical section of another anaphase oocyte with spindle parallel to the cortical surface, and pronounced F-actin deposition between two docked spindle poles. The F-actin pattern of both of these oocytes is similar to that of Fig. 3H, with two centrosome-associated ring centers and increased F-actin deposition appearing principally in the segment between them. Scale bars: 10 μm (bars for B and C as in A).

"late" (Fig. 3D, E), whereas "early" HG addition produced two or more peripheral asters and multiple rings (Fig. 3F–K). Multiple asters and rings were observed more frequently when HG was used in combination with LV than when LV was used alone.

In some of these multiple-ring oocytes, F-actin stained far more intensely in the region between ring openings than in the surrounding area (Fig. 3G, H; confirmed by pixel intensity scanning). When two cortex-associated asters were adjacent and a third more distant, the result was one larger

Figure 3. Hexylene glycol addition during lovastatin metaphase arrest: aster and ring patterns following washout. Optical sections: A, B, C, I; others, rotated 3-D views from image stacks. (A) Enlarged spreading metaphase aster. (B) Two adjacent spreading metaphase asters. (C) Docked metaphase or early anaphase spindle. Inset: higher magnification of two peripheral centrosomes (arrowheads). (D, E) Enlarged rings in late anaphase oocytes, diameters $>$ 30 μm. (F) Pattern variation with one large ring opening containing two docked centrosomes, and a smaller opening with one centrosome. Insets, left: astral pattern; right: associated chromosome sets. (G) F-actin pattern for oocyte in (F), showing major thickening only in shared region between ring openings. (H) Another example of F-actin thickening primarily between ring openings. (I) Oocyte containing three peripherally spread asters (two visible in this section), and three cortical regions of F-actin deposition (arrowheads). (J) Triple ring pattern of same oocyte, with two large ring openings and a third smaller one. (K) Composite view for (J), showing centrosomal regions of the three peripheral asters. Note that ring F-actin deposition is not yet evident in metaphase or early anaphase oocytes (A–C). Scale bar for C inset: 5 μm; others: 10 μm (bar for E as in D; H as in G)

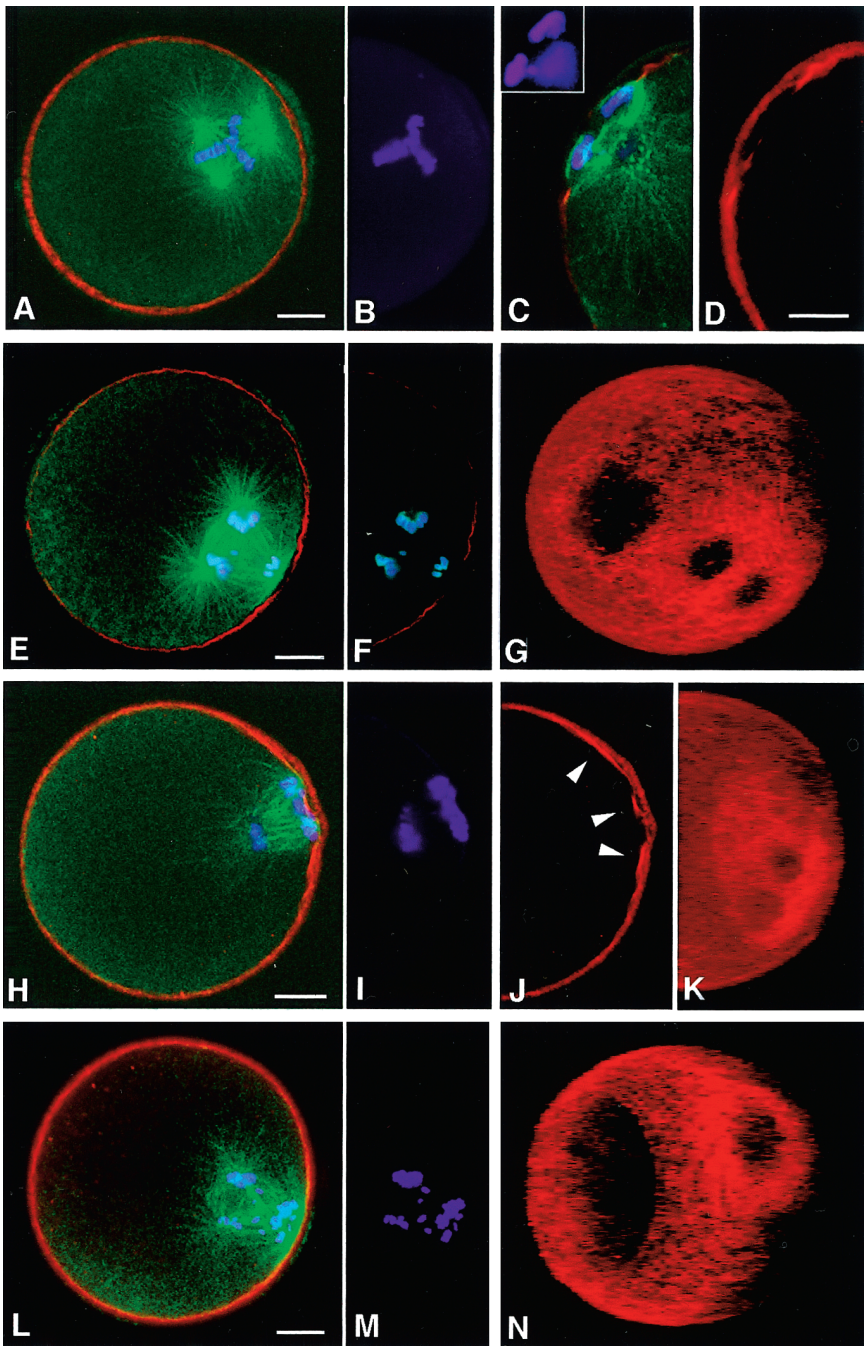

Figure 5. Multiple asters with interconnected spindles and two docked centrosomes, induced by cytochalasin D plus washout. Images (G), (K), and (N) are 3-D views from image stacks; others are optical sections. (A) Multiple spreading metaphase asters, prior to ring formation. (B) Same oocyte, metaphase chromosome sets. (C) Another oocyte at later stage, with two polar bodies extruded after cytochalasin D washout. Inset: chromosome sets, two external and one internal (slight size reduction). (D) Same oocyte as (C), F-actin distribution only. (E) An anaphase oocyte with multiple asters and two centrosomes cortically docked (only one visible in this optical section). (F) Same oocyte as (E), anaphase chromosome sets. (G) Same oocyte, dual cortical F-actin ring pattern. (H) Another anaphase oocyte, with two docked centrosomes. (I) Same oocyte as (H), anaphase chromosome sets. (J) Same oocyte, F-actin pattern only, with three cortical deposition areas (arrowheads). (K) Same oocyte, showing dual cortical F-actin ring pattern. (L) Another anaphase oocyte, with multiple asters, interconnected spindles, and two closely docked centrosomes. (M) Anaphase chromosome sets of same oocyte. (N) Same oocyte, single enlarged, ovoid ring and ring opening. Scale bars: 10 μm (bar for B as in A; C as in D; F and G as in E; I–K as in H; M and N as in L).

ring opening and one smaller one (Fig. 3F, G). However, if centrosomes of three peripherally spread asters were sufficiently separated, three ring openings appeared within a very large region of cortical F-actin deposition (Fig. 3I–K). Despite the unusual ring patterns, about 80%–90% of the oocytes treated with LV plus HG in different preparations ultimately produced PBs after washout, many of which appeared to be larger than control PBs (not shown).

In a minor sub-population of LV-treated oocytes, HG produced single anaphase spindles that were parallel to the cortex, a highly unusual orientation for *Spisula* (Fig. 4). Both centrosomal regions were docked in these oocytes, and two ring openings appeared within a common area of F-actin deposition (Fig. 4A). F-actin deposition was typically intensified between the ring openings (Fig. 4A, C, D), as in some of the multi-aster contact patterns (*e.g.,* Fig. 3G).

Cytochalasin D inhibition of polar body formation, followed by washout

In previous work on shrimp oocytes, cytochalasin blockage of PB1 formation, followed by washout, led to coproduction of two meiotic spindles and two PBs at the time of PB2 formation in controls (Hertzler, 2002). Since this was a potential means to generate two asters in simultaneous cortical contact, and perhaps unusual contact patterns, we tested the approach on *Spisula* oocytes. Cytochalasin effects on *Spisula* PB formation had been investigated earlier, but without such washout (Longo, 1972; Pielak *et al.,* 2004).

Washout of cytochalasin D (CD) (1.0 μg/ml), with controls in early anaphase, was effective in permitting the treated oocytes to proceed into meiosis II. Subsequently, when most controls exhibited a typical metaphase II spindle docked at the cortex, nearly all experimental oocytes contained two or more cortically spreading asters and interconnected metaphase spindles (Fig. 5A, B). Nevertheless, two PBs were ultimately produced at about the same time in these oocytes (Fig. 5C, D). At intermediate anaphase stages, double F-actin rings usually formed, with the two centrosomal regions of the spindles and asters occupying the ring openings (Fig. 5E–K). The dual spindles were sometimes connected at an internal centrosome and docked cortically at an angle to each other (Fig. 5H–K). In several cases, however, two docked anaphase spindles were associated with a single, very large, ovoid F-actin ring (Fig. 5L–N), with both centrosomes occupying the ring center.

Discussion

In the normal cytoskeletal sequence that precedes formation of the polar body (PB) in *Spisula* oocytes, cortical spreading of the peripheral aster at metaphase and cortical docking of the spindle are followed, during anaphase, by disassembly of astral microtubules and formation of the F-actin ring (Fig. 1). The diameters of both aster and ring are typically about 20–22 μm, and the actin-poor center of the ring is similar in dimensions to the microtubule-deficient central region of the earlier spreading aster (Pielak *et al.,* 2003, 2004). These observations suggest that spatial features of PB ring formation are determined by the peripheral aster.

Spatiotemporal relationship between spreading peripheral asters and cortical F-actin rings

In the present work we asked whether altering the number and distribution of peripheral asters would produce corresponding changes in the number and pattern of cortical F-actin rings. The answer was clear: treatment with lovastatin (LV) alone, with LV plus hexylene glycol (HG), or with cytochalasin D (CD), followed by washout, all produced oocytes with multiple cortically spreading peripheral asters (*e.g.,* Figs. 2E; 3B, I; 5E). Subsequently, many of these oocytes produced either a single, abnormally enlarged circular or ovoid ring (>30 μm diameter; *e.g.,* Figs. 2G; 3D, E; 5 N), or multiple overlapping rings (Figs. 2H–J; 3F–K; 5E–K). Single enlarged rings appeared to be generated when centrosomes were in close proximity (*e.g.,* Fig. 2F, G), and this was correlated with considerable increase in astral spreading diameter (long axis of $\approx$40 μm; Fig. 2E). However, it remains to be determined whether both increased microtubule density and astral spreading diameter are critical for cortical F-actin patterning. F-actin thickening between ring openings could be an initial stage of ring biogenesis occurring where overlap of astral microtubules provides the greatest density (*e.g.,* Fig. 3G, H; Fig. 4C, D). Alternatively, thickening could be the result of incomplete cortical contact and spreading by the experimentally altered asters, or a symptom of an additive or even synergistic effect of astral overlap.

With respect to the temporal relationship, F-actin rings were observed in normal oocytes only in anaphase (Fig. 1). Oocytes exposed to LV, or LV plus HG, completed astral spreading and spindle docking, but were arrested at metaphase due to blockage of the degradation of *Spisula* oocyte cyclin A and B (Hunt *et al.,* 1992; Turner *et al.,* 1995). F-actin rings were not generated unless the drugs were washed out, permitting entry into anaphase (Fig. 2F; 4A). In addition, after CD-washout, multiple F-actin rings were observed only in anaphase cells (Fig. 5A, B *vs.* 5E, F). Therefore, both astral contact and anaphase-triggered events must determine biogenesis of the F-actin ring for *Spisula* PB formation. This is consistent with the importance of anaphase entry for somatic furrowing, as evident in early work on echinoderm zygotes whose asters had been removed or disrupted (Cornman and Comman, 1951; Swann and Mitchison, 1953; Mitchison, 1953; Scott, 1960), and in later studies on the appearance of actin filament bundles in the cortex (Mabuchi, 1994).

Function of asters versus centrosomal regions

The experimentally generated rings exhibited various patterns, most of which can be accounted for by varying degrees of ring overlap following a stimulus from the astral microtubules (Fig. 6A–E). However, we observed no ring openings "filled in" by F-actin from an adjacent ring (Fig. 6F, G). This cannot be explained simply by stimulus reduction caused by low microtubule density at adjacent astral centers, and therefore we suggest that, in contrast to astral microtubules, docked centrosomes may inhibit F-actin deposition. Such a mechanism would ensure reduction of mechanical resistance in ring openings, the cortical site of PB extrusion. Adjacent centrosomes would then produce one enlarged ring opening (*e.g.,* Figs. 2G; 3G; 5N); if the centrosomes were further apart, multiple ring openings would be surrounded by F-actin from overlapping rings (*e.g.,* Fig. 2H–J; 3F–K; 5G). The centrosomes of spindles abnormally docked parallel to the cortex would be separated by the spindle itself, generating separate ring openings (Fig. 4A–C). While we find no published evidence for or against such speculation, it is worth noting that centrosomes isolated from *Spisula* oocytes, though too small ($\approx$2 μm diameter) for simple obstruction of ring openings, contain a great many proteins of unknown function (Palazzo and Vogel, 1999).

In the androgenetic bivalve *Corbicula,* two PBs are produced naturally after simultaneous spreading of two metaphase I asters. Here, the metaphase I spindle always aligns parallel to the oocyte surface, and both asters spread cortically prior to dual PB extrusion (Komaru *et al.,* 2000). This differs from CD-washout, in which dual anaphase II spindles appear nearly end-on to the cortex (Fig. 5H), but it resembles the parallel spindle-cortex alignment in oocytes treated with LV plus HG, generating dual overlapping rings (Fig. 4). The actual F-actin ring pattern in *Corbicula* has not yet been determined, however.

Mechanisms involved in multiple aster and ring generation

Multiple and enlarged asters and rings occurred after treatment and washout using LV, LV plus HG, or CD (Figs. 2–5). Since different means produced the same general result, multiple ring formation is aster-related, not drug-related. Multiple asters were expected for treatment with CD but not with LV; the latter may reflect use at a somewhat higher concentration and temperature than in earlier work (Turner *et al.,* 1995). Although knowledge of the specific mechanisms that produce multiple asters is not critical to present conclusions, we believe centrosome replication to be responsible in both cases. Typical meiotic events continue during CD inhibition of ring and PB1 formation in *Spisula* (Pielak *et al.,* 2004), and, in the case of LV, centrosome replication and separation apparently proceed during the metaphase block or shortly after washout (Fig. 3C).

Since astral perturbation produced marked pattern alterations, the biogenetic signal or mechanism for F-actin deposition must be recognized indiscriminately by the *Spisula* oocyte cortex (Fig. 7). In other species, such ring induction would account for PB formation at different cortical sites after experimental translocation of the meiotic apparatus (Hamaguchi *et al.,* 2001), and for an indiscriminate furrowing response in somatic cytokinesis (Kawamura, 1960; Rappaport, 1985). In normal *Spisula* oocytes, the circular cortical F-actin ring and ring opening occupy nearly 40% of oocyte diameter before PB extrusion (Fig. 1E), but we do not yet know whether other invertebrates exhibit this ring pattern and size (Shimizu, 1990; Hamaguchi *et al.,* 2001).

Do astral microtubules simply provide signals marking cortical regions, or do they deliver F-actin and other ring components? This question remains open both for *Spisula* oocytes and for PB formation. In several other systems there is evidence that microtubules determine F-actin distribution

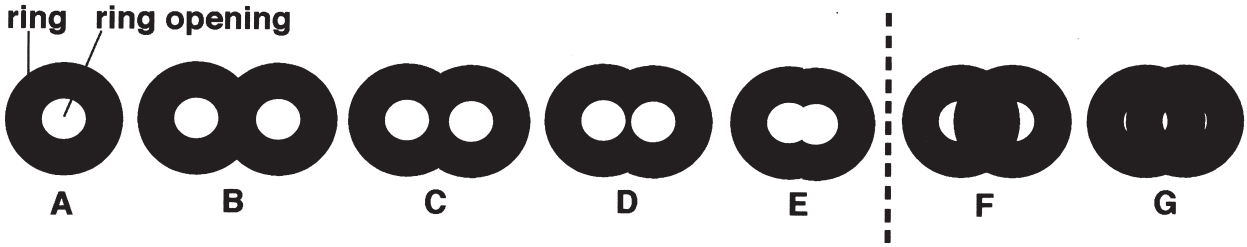

Figure 6. Diagram of pattern variations in dual rings and ring openings. (A) Ring pattern generated during normal (control) polar body biogenesis, or enlarged in cells treated with lovastatin plus hexylene glycol (Figs. 1E; 3D, E). (B) Partial overlap of adjacent rings (Figs. 2H; 5G). (C, D) Progressively greater ring overlap patterns (Figs. 2I, J; 3F). (E) Marked overlap, such that ring openings are joined (Figs. 2G; 5N). (F, G) Patterns of overlap that were not observed. Absence of such patterns indicates that, whereas the earlier spreading astral microtubules have a stimulatory effect on F-actin deposition, each docked spindle or centrosome thereof, occupying a ring center, has an inhibitory influence. This would prevent neighboring spread asters from inducing F-actin deposition in the adjacent ring opening. Patterns such as those in (A–E) can then be accounted for based on the distance between spreading asters and the centrosomes of their docked spindles.

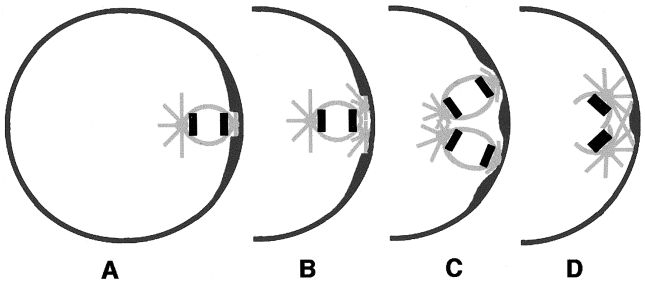

Figure 7. Schematic of observed F-actin patterns in relation to docked spindles and their centrosomal regions. (A) Single circular ring (Figs. 1E; 3D, E). (B) Large ovoid ring (Figs. 2G; 5N). (C) Double ring (Figs. 2H–J; 3G, H; 5H–K). (D) Spindle parallel to cortex, F-actin between centrosomes (Fig. 4B, C). The variations in size, pattern, and location demonstrate that the cortex responds indiscriminately to the astral influence.

and furrow position (grasshopper spermatocytes: Alsop and Zhang, 2004), addition of new furrow membrane (sea urchin zygotes: Shuster and Burgess, 2002), and furrow induction *via* transported proteins (mammalian cells: Canman *et al.,* 2003); in addition, direct actin-microtubule interaction has been reported in *Drosophila embryos* and *in vitro* (Sider *et al.,* 1999; Foe *et al.,* 2000; Waterman-Storer *et al.,* 2000). With respect to PB ring signaling in *Spisula* oocytes, Rho is a good candidate for study. Rho family GTPases are believed to determine properties of F-actin rings involved in somatic cytokinesis and oocyte wound-healing (Mabuchi *et al.,* 1993; Nishimura *et al.,* 1998; Saint and Somers, 2003; Somers and Saint, 2003; Yonemura *et al.,* 2004; Benink and Bement, 2005).

Regardless of molecular mechanism, peripheral asters clearly function to induce F-actin rings associated with PB extrusion in *Spisula.* Thus, at the cellular level at least, PB biogenesis in *Spisula* differs from that in mammals. The mammalian meiosis I spindle has truncated asters (Szollosi *et al.,* 1972), and cortical spindle positioning involves actin filaments and formin-2 rather than astral microtubules (Leader *et al.,* 2002; Maro and Verlhac, 2002). Comparison of the pathways to PB formation taken by mammalian, non-mammalian vertebrate, and invertebrate oocytes would be of considerable interest, and *Spisula* provides an excellent model system for such work.

Note added in proof: Evidence for RhoA involvement in establishing the polar body F-actin ring in *Xenopus,* as well as somatic contractile rings in echinoderms, is provided in a new paper by Bement *et al.* (2005).

Acknowledgments

We are indebted to Louie Kerr of the MBL and Rudi Rottenfusser of Carl Zeiss Inc. for the excellent confocal microscopy facilities, and to the Howard Hughes Medical Institute Undergraduate Science Education Program in Biology (HHMI 5200267), the Hunter College Avon-Tukman Fund, NSF 9808368, and PSC-CUNY 65218, for support.

Literature Cited

Allen, R. D. 1953. Fertilization and artificial activation in the egg of the surf-clam, *Spisula solidissima. Biol. Bull.* **105:** 213–239.

Alliegro, M. C., and M. A. Alliegro. 2005. Differential expression of tyrosinated tubulin in *Spisula solidissima* polar bodies. *Dev. Dyn.* **232:** 216–220.

Alsop, G. B., and D. Zhang. 2004. Microtubules continuously dictate distribution of actin filaments and positioning of cell cleavage in grasshopper spermatocytes. *J. Cell Sci.* **117:** 1591–1602.

Bement, W. M., H. A. Benink, and G. von Dassow. 2005. A microtubule-dependent zone of active RhoA during cleavage plane specification. *J. Cell Biol.* **170** (in press).

Benink, H. A., and W. M. Bement. 2005. Concentric zones of active RhoA and Cdc42 around single cell wounds. *J. Cell Biol.* **168:** 429–439.

Canman, J. C., L. A. Cameron, P. S. Maddox, A. Straight, J. S. Tirnauer, T. J. Mitchison, G. Fang, T. M. Kapoor, and E. D. Salmon. 2003. Determining the position of the cell division plane. *Nature* **424:** 1074–1078.

Castro, A., E. Mandart, T. Lorca, and S. Galas. 2003. Involvement of Aurora A kinase during meiosis I–II transition in *Xenopus* oocytes. *J. Biol. Chem.* **278:** 2236–2241.

Cornman, I., and M. E. Cornman. 1951. The action of podophyllin and its fractions on marine eggs. *Ann. N.Y. Acad. Sci.* **51:** 1443–1487.

Costello, D. P., and C. Henley. 1971. *Methods for Obtaining and Handling Marine Eggs and Embryos. Mollusca:* Mactra solidissima, 2nd ed. Marine Biological Laboratory, Woods Hole, MA. Also available at: http://www.mbl.edu/BiologicalBulletin/CLASSICS/COSTELLO/index.html [accessed 12 March 2005].

Dessev, G., and R. Goldman. 1988. Meiotic breakdown of nuclear envelope in oocytes of *Spisula solidissima* involves phosphorylation and release of nuclear lamin. *Dev. Biol.* **1302:** 543–550.

Dessev, G., R. Palazzo, L. Rebhun, and R. Goldman. 1989. Disassembly of the nuclear envelope of *Spisula* oocytes in a cell-free system. *Dev. Biol.* **1312:** 496–504.

Dubé, F., and W. R. Eckberg. 1997. Intracellular pH increase driven by an Na^+/H^+ exchanger upon activation of surf clam oocytes. *Dev. Biol.* **190:** 41–54.

Foe, V. E., C. M. Field, and G. M. Odell. 2000. Microtubules and mitotic cycle phase modulate spatiotemporal distributions of F-actin and myosin II in *Drosophila* syncytial blastoderm embryos. *Development* **127:** 1767–1787.

Haimo, L. T. 1985. Microtubule polarity in taxol-treated isolated spindles. *Can. J. Biochem. Cell. Biol.* **63:** 519–532.

Hamaguchi, Y., S. K. Satoh, T. Numata, and M. S. Hamaguchi. 2001. Response of the cortex to the mitotic apparatus during polar body formation in the starfish oocyte of *Asterina pectinifera. Cell Struct. Funct.* **2:** 627–631.

Hertzler, P. L. 2002. Twin meiosis 2 spindles form after suppression of polar body 1 formation in oocytes of the marine shrimp *Sicyonia ingentis. Biol. Bull.* **202:** 100–103.

Hunt, T., F. C. Luca, and J. V. Ruderman. 1992. The requirements for protein synthesis and degradation, and the control of destruction of cyclins A and B in the meiotic and mitotic cell cycles of the clam embryo. *J. Cell Biol.* **116:** 707–724.

Katsu, Y., N. Minshall, Y. Nagahama, and N. Standart. 1999. Ca^{2+} is required for phosphorylation of clam p82/CPEB *in vitro:* implications for dual and independent roles of MAP and Cdc2 kinases. *Dev. Biol.* **209:** 186–199.

Kawamura, K. 1960. Studies on cytokinesis in neuroblasts of the grasshopper, *Chortophaga viridifasciata* (de Geer). II. The role of the mitotic apparatus in cytokinesis. *Exp. Cell Res.* **21:** 9–18.

Komaru, A., K. Ookubo, and M. Kiyomoto. 2000. All meiotic chromosomes and both centrosomes at spindle pole in the zygotes discarded as two polar bodies in clam *Corbicula leana:* unusual polar body

formation observed by antitubulin immunofluorescence. *Dev. Genes Evol.* **210:** 263–269.

Kuriyama, R., G. G. Borisy, and Y. Masui. 1986. Microtubule cycles in oocytes of the surf clam, *Spisula solidissima:* an immunofluorescence study. *Dev. Biol.* **114:** 151–160.

Leader, B., H. Lim, M. J. Carabatsos, A. Harrington, J. Ecsedy, D. Pellman, R. Maas, and P. Leder. 2002. Formin-2, polyploidy, hypofertility and positioning of the meiotic spindle in mouse oocytes. *Nat. Cell Biol.* **4:** 921–928.

Lee, K. G., A. Braun, I. Chaikhoutdinov, J. DeNobile, M. Conrad, and W. Cohen. 2002. Rapid visualization of microtubules in blood cells and other cell types in marine model organisms. *Biol. Bull.* **203:** 204–206.

Longo, F. J. 1972. The effects of cytochalasin B on the events of fertilization in the surf clam, *Spisula solidissima.* I. Polar body formation. *J. Exp. Zool.* **182:** 321–344.

Longo, F. J., and E. Anderson. 1970. An ultrastructural analysis of fertilization in the surf clam, *Spisula solidissima.* I. Polar body formation and development of the female pronucleus. *J. Ultrastruct. Res.* **33:** 495–514.

Longo F. J., S. Cook, L. Mathews, and S. J. Wright. 1991. Nascent protein requirement for completion of meiotic maturation and pronuclear development: examination of fertilized and A-23187-activated surf clam (*Spisula solidissima*) eggs. *Dev. Biol.* **148:** 75–86.

Mabuchi, I. 1994. Cleavage furrow: timing of emergence of contractile ring actin filaments and establishment of the contractile ring by filament bundling in sea urchin eggs. *J. Cell Sci.* **107:** 1853–1862.

Mabuchi, I., Y. Hamaguchi, H. Fujimoto, N. Morii, M. Mishima, and S. Narumiya. 1993. A rho-like protein is involved in the organisation of the contractile ring in dividing sand dollar eggs. *Zygote* **1:** 325–331.

Marine Biological Laboratory. 2003. Clam mini-genome project. Pp. 1–2 in *LabNotes,* vol. 14, no. 1. Also available at: http://www.mbl.edu/inside/what/news/publications/labnotes/04_spring.html [accessed 12 March 2005].

Maro, B., and M. H. Verlhac. 2002. Polar body formation: new rules for asymmetric divisions. *Nat. Cell Biol.* **4:** 921–928.

Maul, G. G., G. Schatten, S. A. Jimenez, and A. E. Carrera. 1987. Detection of nuclear lamin B epitopes in oocyte nuclei from mice, sea urchins, and clams using a human autoimmune serum. *Dev. Biol.* **1212:** 368–375.

Mitchison, J. M. 1953. Microdissection experiments on sea-urchin eggs at cleavage. *J. Exp. Biol.* **30:** 515–526.

Nishimura, Y., K. Nakano, and I. Mabuchi. 1998. Localization of Rho GTPase in sea urchin eggs. *FEBS. Lett.* **441:** 121–126.

Palazzo, R. E., and J. M. Vogel. 1999. Isolation of centrosomes from *Spisula solidissima* oocytes. *Methods Cell Biol.* **61:** 35–56.

Pielak, R. M., V. A. Gaysinskaya, and W. D. Cohen. 2003. Cytoskeletal events preceding polar body formation in activated *Spisula* eggs. *Biol. Bull.* **205:** 192–193.

Pielak R. M., V. A. Gaysinskaya, and W. D. Cohen. 2004. Formation and function of the polar body contractile ring in *Spisula. Dev. Biol.* **269:** 421–432.

Rappaport, R. 1985. Repeated furrow formation from a single mitotic apparatus in cylindrical sand dollar eggs. *J. Exp. Zool.* **234:** 167–171.

Rebhun, L. I., and N. Sawada. 1969. Augmentation and dispersion of the in vivo mitotic apparatus of living marine eggs. *Protoplasma* **68:** 1–22.

Saiki, T., and Y. Hamaguchi. 1997. Division of polar bodies induced by their enlargement in the starfish *Asterina pectinifera. Exp. Cell Res.* **237:** 142–148.

Saint, R., and W. G. Somers. 2003. Animal cell division: a fellowship of the double ring? *J. Cell Sci.* **116:** 4277–4281.

Schnackenberg, B. J., D. R. Hull, R. D. Balczon, and R. E. Palazzo. 2000. Reconstitution of microtubule nucleation potential in centrosomes isolated from *Spisula solidissima* oocytes. *J. Cell Sci.* **113:** 943–953.

Schumacher, J. M., A. Golden, and P. J. Donovan. 1998. AIR-2: An Aurora/Ip11-related protein kinase associated with chromosomes and midbody microtubules is required for polar body extrusion and cytokinesis in *Caenorhabditis elegans* embryos. *J. Cell Biol.* **143:** 1635–1646.

Scott, A. C. 1960. Furrowing in flattened sea urchin eggs. *Biol. Bull.* **119:** 246–259.

Shimizu, T. 1990. Polar body formation in *Tubifex* eggs. Pp. 260–272 in *Cytokinesis:* Mechanisms of Furrow Formation During Cell Division, G. W. Conrad and T. E. Schroeder, eds. New York Academy of Sciences, New York.

Shuster, C. B., and D. R. Burgess. 2002. Targeted new membrane addition in the cleavage furrow is a late, separate event in cytokinesis. *Proc. Natl. Acad. Sci. USA* **99:** 3633–3638.

Sider, J. R., C. A. Mandato, K. L. Weber, A. J. Zandy, D. Beach, R. J. Finst, J. Skoble, and W. M. Bement. 1999. Direct observation of microtubule-F-actin interaction in cell free lysates. *J. Cell Sci.* **112:** 1947–1956.

Somers, W. G., and R. A. Saint. 2003. RhoGEF and Rho family GTPase-activating protein complex links the contractile ring to cortical microtubules at the onset of cytokinesis. *Dev. Cell* **4:** 29–39.

Suddith, A. W., E. A. Vaisberg, S. A. Kuznetsov, W. Steffen, C. L. Rieder, and R. E. Palazzo. 2001. Centriole duplication, centrosome maturation and spindle assembly in lysates of *Spisula solidissima* oocytes. *Methods Mol. Biol.* **161:** 215–228.

Suprenant K. A., and L. I. Rebhun. 1984. Purification and characterization of oocyte cytoplasmic tubulin and meiotic spindle tubulin of the surf clam *Spisula solidissima. J. Cell Biol.* **98:** 253–266.

Swann, M. M., and J. M. Mitchison. 1953. Cleavage of sea-urchin eggs in colchicine. *J. Exp. Biol.* **30:** 506–514.

Swenson, K. I., N. Borgese, G. Pietrini, and J. V. Ruderman. 1987. Three translationally regulated mRNAs are stored in the cytoplasm of clam oocytes. *Dev. Biol.* **123:** 10–16.

Szollosi, D., P. Calarco, and R. P. Donahue. 1972. Absence of centrioles in the first and second meiotic spindles of mouse oocytes. *J. Cell Sci.* **11:** 521–541.

Turner, J. E., C. G. Minkoff, K. H. Martin, R. Misra, and K. I. Swenson. 1995. Oocyte activation and passage through the metaphase/anaphase transition of the meiotic cell cycle is blocked in clams by inhibitors of HMG-CoA reductase activity. *J. Cell Biol.* **128:** 1145–1162.

Waterman-Storer, C., D. Y. Duey, K. L. Weber, J. Keech, R. E. Cheney, E. D. Salmon, and W. M. Bement. 2000. Microtubules remodel actomyosin networks in *Xenopus* egg extracts via two mechanisms of F-actin transport. *J. Cell Biol.* **150:** 361–376.

Weinberg, J. R., and T. E. Helser. 1996. Growth of the Atlantic surfclam, *Spisula solidissima,* from Georges Bank to the Delmarva peninsula, USA. *Mar. Biol.* **126:** 663–674.

Wu, X., and R. E. Palazzo. 1999. Differential regulation of maternal vs. paternal centrosomes. *Proc. Natl. Acad. Sci. USA* **96:** 1397–1402.

Yi, J.-H., L. Lefièvre, C. Gagnon, M. Anctil, and F. Dubé. 2002. Increase of cAMP upon release from prophase arrest in surf clam oocytes. *J. Cell Sci.* **115:** 311–320.

Yonemura, S., K. Hirao-Minakuchi, and Y. Nishimura. 2004. Rho localization in cells and tissues. *Exp. Cell Res.* **295:** 300–314.